

Molecular Size Determination of Coal-Derived Asphaltene by Fluorescence Correlation Spectroscopy

A. BALLARD ANDREWS,* WEI-CHUAN SHIH, OLIVER C. MULLINS,
and KOYO NORINAGA

Schlumberger-Doll Research, Cambridge, Massachusetts 02139 (A.B.A., W.-C.S., O.C.M.); Hokkaido University, Sapporo, Japan (K.N.); and Electrical and Computer Engineering Dept., University of Houston, Houston, Texas 77004 (W.-C.S.)

The molecular properties of asphaltenes have been the subject of uncertainty in the literature; in particular the molecular architecture is still a matter of debate. Some literature reports provide evidence that the contrast of petroleum asphaltenes versus coal-derived asphaltenes is useful for understanding the governing principles of asphaltene identity. Here, we employ fluorescence correlation spectroscopy to measure the diffusion constants of asphaltenes obtained from the distillation resid from coal liquefaction fluids. Concentrations employed herein are $\sim 10^{-8}$ molar, precluding asphaltene aggregation. These are compared with the same measurements on petroleum asphaltenes. These results confirm that the molecular sizes of these coal-derived asphaltenes are much smaller than virgin petroleum asphaltenes. Coal-derived asphaltenes are simpler than petroleum asphaltenes and provide correspondingly tighter constraints for understanding asphaltene molecular architecture. The small size, small alkane fraction, and large PAH of coal-derived asphaltenes are consistent with an "island" molecular architecture.

Index Headings: **Asphaltenes; Fluorescence correlation spectroscopy; Diffusion.**

INTRODUCTION

Asphaltenes have been the subject of numerous studies, but often with vastly differing conclusions. Fortunately, there has been convergence on several fundamental properties of asphaltenes.^{1–3} A new representation of asphaltenes consisting of explicit structures of asphaltene molecules, nanoaggregates, and clusters builds on the pioneering work of Yen and is called the "modified Yen Model,"^{2,3} incorporating the bulk of recent advances. Asphaltene molecular weight is for the most part no longer a controversial subject. Four different diffusion measurements have been employed to examine asphaltene molecular size and thus asphaltene molecular weight. Time-resolved fluorescence depolarization (TRFD) has been used to measure the rotational diffusion constants of asphaltenes from petroleum,^{4,5} coals,^{6,7} thermally processed feedstock,⁷ and solubility subfractions of petroleum asphaltenes.^{8,9} The TRFD results show that (1) asphaltenes are relatively small in molecular size and (2) that asphaltenes consist of molecules primarily with one fused ring system per molecule. Taylor dispersion diffusion measurements which relied on optical absorption measurements to determine the translational diffusion constant of a coal-derived asphaltene (the same sample as the TRFD study) found excellent agreement with the TRFD results.¹⁰ Nuclear magnetic resonance (NMR) pulsed field gradient measurements were employed on petroleum asphaltenes and again obtained reasonable agreement with the TRFD

studies for the same samples.¹¹ One difference is that the NMR studies exhibited a somewhat larger high mass tail, but then again the minimum concentration used for these studies was 50 mg/liter in toluene where asphaltenes have been shown to dimerize.^{9,12} Indeed, at somewhat higher concentrations (~ 150 mg/liter in toluene) asphaltenes have been shown to form nanoaggregates; consistent results have been obtained by high-Q ultrasonics,^{13,14} NMR,¹¹ AC conductivity,¹⁵ DC conductivity,^{16,17} and corroborated by centrifugation studies.^{18,19} Moreover, the critical nano-aggregate concentration (CNAC) obtained by centrifugation has been shown on the same samples to coincide with that obtained by high-Q ultrasonics¹⁹ and by DC conductivity¹⁸ for the same asphaltene samples.

Fluorescence correlation spectroscopy (FCS) has proved very useful in the study of asphaltene diffusion constants.^{20–22} FCS on asphaltenes is performed at extremely low concentrations with mass fractions typically at 10^{-7} but as low as 10^{-8} ($\sim 10^{-8}$ M), which is far below dimer and nanoaggregate concentrations reported elsewhere.^{9,12–15} No dependence on concentration of FCS results has been observed in this concentration range.²² Therefore, there is no question that the FCS experiments on asphaltenes are performed on individual molecules in solution. In addition, FCS enables direct comparison of results with TRFD to rule out possible intramolecular rotational relaxation artifacts in TRFD data. Since FCS measures translational diffusion at the micron length scale, there is no possibility of intra-molecular diffusion interfering with FCS interpretation. The strong agreement between TRFD and FCS diffusion results reinforces TRFD conclusions; there are no detectable intra-molecular relaxation artifacts. The FCS results are very amenable to stringent theoretical analysis, both with regard to the explicit functional form of the autocorrelation relaxation curve as well as dependencies on experimental parameters such as temperature. Our FCS instrument produces autocorrelation curves that are indistinguishable from the theoretical curves, lending credence to the robustness and accuracy of the measurements.²² In addition, a very broad range of model compounds and fluorescent species including quantum dots have been run, establishing the validity of the FCS approach.^{20–22}

The primary result of all asphaltene diffusion measurements in general and certainly the FCS results in particular is that asphaltene molecules are small. In large measure, when the first TRFD results were published, the conventional wisdom at the time was that asphaltene molecules are polymeric and well in excess of 1000 Da. The diffusion measurements have played a major role in changing this perspective. Boduszynski published field ionization mass spectral results that concluded that the bulk of asphaltenes are under a kilodalton.²³ These results, which are in good agreement with the diffusion measurements, were somewhat discounted with the general complaint that (1)

Received 8 February 2011; accepted 29 September 2011.

* Author to whom correspondence should be sent. E-mail: bandrews@slb.com.

DOI: 10.1366/11-06258

fragmentation “must” be occurring and (2) the heaviest species are not being desorbed. In recent years there has been extensive use of electrospray ionization (ESI), a technique that is known to be quite soft; it does not result in fragmentation. Fenn and others have made use of ESI on crude oils with results consistent with diffusion measurements.²⁴

Electrospray ionization coupled with Fourier transform ion cyclotron resonance mass spectroscopy has been applied to petroleum asphaltene fractions.^{25–27} The results of ESI FT-ICR MS are in very close agreement with all asphaltene diffusion measurements.²⁸ Earlier laser desorption ionization (LDI) studies had found evidence of large molecular weights at higher laser power.²⁹ However, subsequent LDI work on asphaltenes showed that gas-phase aggregation can dominate LDI results on asphaltenes if the corresponding plasma is too dense.^{30–32} High laser power, high surface asphaltene concentration, or even rapid ion extraction after plasma formation can all yield extensive gas-phase aggregation.^{30–32} Strong support for the claims of artifactual gas-phase aggregation have been obtained in two-step laser desorption/ionization (L²MS), wherein an infrared (IR) laser is used to desorb neutral asphaltenes, with their much lower tendency to aggregate than ions, and a second laser, a UV laser, performs the ionization.^{33–35}

These experiments show independence of measured asphaltene molecular weight on IR laser power, UV laser power, or laser pulse timing.^{33,34} In fact, the IR laser power per unit area employed in these asphaltene studies greatly exceeds that employed in single-color LDI, which had yielded large asphaltene “molecules”, proving that the supposedly large molecules were actually aggregates formed in the gas phase. In addition, laser-induced acoustic desorption electron impact (LIAD-EI) mass spectrometry reports most probable asphaltene molecular weight of 750 Da, exactly in agreement with the diffusion and other measurements.^{36,37} Results from field desorption mass spectrometry yield somewhat larger masses for petroleum asphaltenes (~1 kDa) but are still close to other determinations.

The first primary result from the diffusion studies is that asphaltene molecular weight is roughly 750 Da with 500 to 1000 Da full width at half-maximum (FWHM). The second primary result of the diffusion measurements (TRFD) is that there are one or perhaps two polycyclic aromatic hydrocarbons (PAHs) per molecule, a result which has also been controversial. There is recent support for this finding from single-molecule decomposition studies.^{35,37,38} Independent of whether asphaltenes are decomposed by electron impact,³⁵ photo-absorption,³⁷ or He atom collision,³⁸ the result is always the same; only island molecular architecture is found for asphaltenes. Additionally, an examination of PAHs coupled with spectral analysis of asphaltenes supports this finding.^{39–41} Also note that a seven-ring PAH with ~50% alkane carbon and a heteroatom or two yields a mass of ~750 Da. Thus, if seven ring PAHs are the most probable, as claimed,^{4–9,39–41} then a single PAH per molecule is exactly consistent with the now known molecular weights of asphaltenes.

The importance of this finding, predominantly one PAH per asphaltene molecule, is immediately felt in interfacial studies. Sum frequency generation (SFG) measurements have been used to perform the first direct measurement of asphaltene molecular orientation in Langmuir–Blodgett films.⁴² The very high degree of alignment of asphaltene PAHs in the plane of the interface and the very high degree of orientation of asphaltene alkanes perpendicular to the interface is consistent

only with the island architecture and not the archipelago model.⁴² In addition, the island model compounds are also highly oriented, again supporting island molecular architecture for asphaltenes. These SFG experiments provide the foundation of the first principles approach to petroleum interfacial science and represent a powerful advance.

Asphaltenes are defined as a solubility class dissolving in toluene and precipitating in *n*-heptane. A simple model has been put forth to explain a variety of results from asphaltenes. The idea is that asphaltene molecular identity is defined by a balance of intermolecular attraction versus repulsion. The PAH ring systems provide attraction via van der Waals forces, while the alkanes yield steric repulsion (and especially interfere with stacking in the solid.⁶ A larger (single) PAH yields more attraction and more alkane carbon yields more repulsion. To test this idea, coal-derived asphaltene has been contrasted with petroleum asphaltenes. The coal-source material is deficient of hydrogen and the distillation of coal liquids yields further loss of alkane (and functional groups). Indeed, ¹³C NMR on a coal-derived asphaltene showed that the coal-derived asphaltene has a much higher fraction of aromatic carbon than the petroleum asphaltene.⁴³ These NMR studies show that coal PAHs are fairly large, with 5 to 6 fused rings on average. Coal-derived asphaltenes have been shown to be half the size of many crude oil asphaltenes by LDI,³² and L²MS.³³ The small size, small alkane fraction, and large PAH of coal-derived asphaltenes is consistent with predominant island molecular architecture.

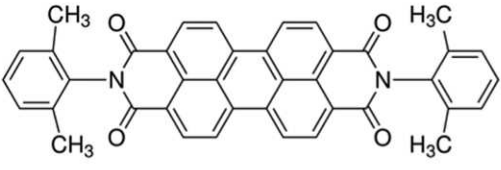
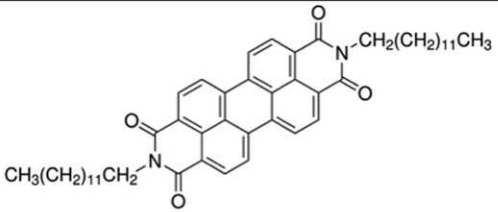
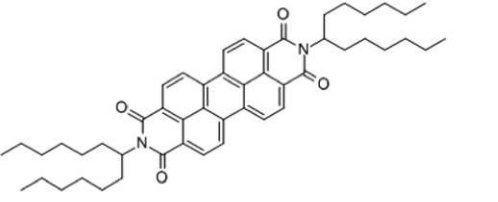
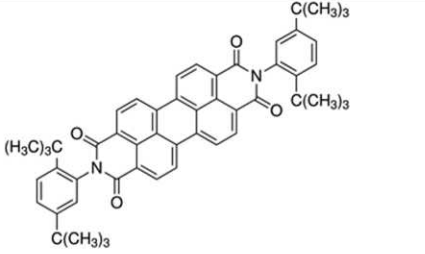
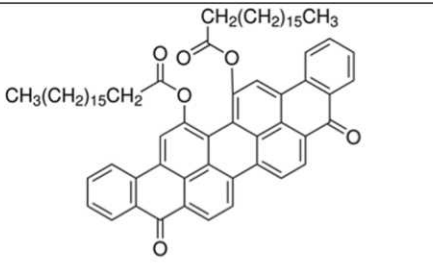
Indeed similar reasoning has been used to determine (natural) dissolved organic matter (DOM) in the oceans. It has been established that at least some of the heavy DOM is associated with natural oil seeps.^{44–46} The heavy DOM appears to be biodegraded asphaltenes where the alkane substitution has been largely consumed, leaving an aromatic core, little alkane carbon, and some carboxylic acid groups (making this material water soluble).^{44–46} These compounds often have a single, large PAH (~7 rings).⁴⁶ Similar to our approach with coal-derived asphaltenes, the small molecular weight and the very small alkane fraction is compelling that the DOM has the island architecture;⁴⁶ we take the same approach for coal-derived asphaltenes.

In this paper, three coal-derived asphaltenes are prepared each from the resid of a vacuum distillation of the corresponding liquefaction fraction from a particular coal. FCS measurements were performed on four coal-liquefaction resid asphaltenes. These coal data are compared to four known petroleum asphaltenes and several PAH model compounds by the same FCS setup. In a separate publication these coal-derived samples have been characterized by ¹³C NMR and distortionless enhancement by polarization transfer (DEPT) methods to provide robust analysis of key molecular structure issues, particularly the saturate to aromatic carbon ratio.⁴³ The relationship between diffusion and molecular structure is stressed. Coal-derived asphaltenes have smaller molecular weights, smaller alkane fractions and somewhat smaller PAHs than petroleum asphaltenes.⁴³ The analysis of the coal-derived asphaltenes is straightforward; the data is consistent with only one PAH per molecule.

EXPERIMENTAL

Three different coal-derived asphaltenes were studied, two from Indonesia, Tanito Harum (TH) and Adaro (AD), and one from the United States, Wyoming (WY). These coals were

Table I. Fluorescent dyes used as model compounds for this study.

Full Name (Abbr.)	Molecular Structure	Molecular weight (Da)
N,N'-Bis(2,6-dimethylphenyl) perylene-3,4,9,10-tetracarboxylic diimide (BPTD)		598.65
N,N'-Ditridecylperylene-3,4,9,10-tetracarboxylic diimide (Solar)		755.04
N,N'-bis(1-hexylheptyl)-perylene-3,4:9,10-bis-(dicarboximide) (BHPD)		755.04
N,N'-Bis(2,5-di-tert-butylphenyl)-3,4,9,10-perylenedicarboximide (BPTI)		766.96
Violanthrone-78 (PTP)		1021.41

liquefied, these liquids distilled, and the distillation resid was then extracted to obtain coal-derived asphaltenes. Note that the FCS experiments are sensitive only to the fraction of sample that absorbs light, here 515 nm (green).

In addition, multiple preparations of one coal-derived asphaltene, Tanito Harum, were analyzed in order to compare all previous work on this material with the samples analyzed for the first time herein. The previous preparation TH-coal-derived asphaltene was initially prepared by Iino¹⁰ using the mixed solvent system NMP-CS₂. The end of the solvent extraction gave a toluene soluble, n-heptane insoluble fraction (and thus an asphaltene), but the process differed from a

straight toluene extraction from the resid employed on all coal-derived asphaltene samples here. Comparison of the TH-coal-derived asphaltene with that using the Iino preparation compares both reproducibility and dependence of results on the exact extraction process.

Four petroleum-derived asphaltenes were studied with FCS (CAL, UG8, BG5, and STO). In order to establish a comparative scale for the asphaltene diffusion times, a selection of different model compounds was measured. A list of these dyes with the full names and abbreviations used in the paper, chemical structure, and molecular weights are given in Table I. The perylene derivatives BPTD, Solar-dye, BPTI and

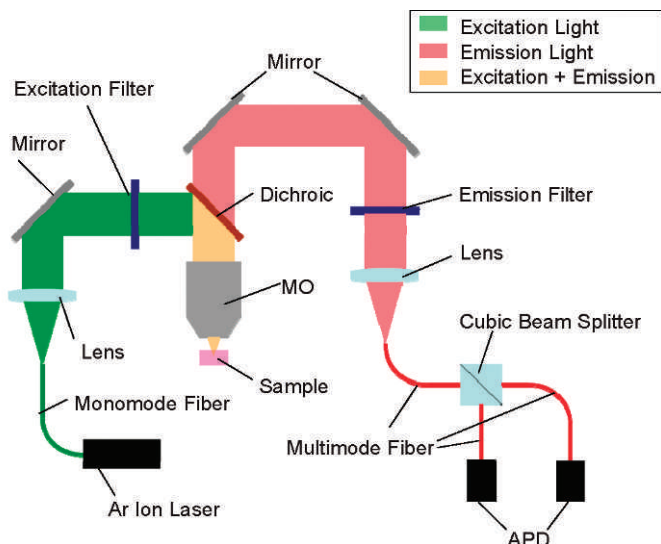


FIG. 1. Schematic of the FCS microscope. The 515 nm Ar laser is coupled via a single-mode fiber to the optical train and collimated to underfill the back aperture of the 60 \times objective. Cross-correlation is obtained with a beam splitter and two avalanche photodiodes (APDs).

BHPD are molecules with a similar aromatic ring core system but different sized substituents, while the Violanthrone perylene derivative has a nine-ring aromatic core and long aliphatic side chains.

Fluorescence Correlation Spectroscopy. FCS extracts information from the spontaneous fast fluctuations that appear as noise in traditional fluorescence measurements by quantifying their strength and duration with temporal autocorrelation of the recorded intensity signal. The fluctuations result from fluorescent molecules diffusing into or out of the interrogated focal volume in the FCS microscope. These fluctuations in the fluorescence signal are expressed as:⁴⁷

$$\delta F(t) = \xi \int_V W(\vec{r}) \delta C(\vec{r}, t) dV \quad (1)$$

where $W(\vec{r})$ is the normalized point spread function (PSF) of the microscope and $\delta C(\vec{r}, t)$ describes the local concentration of the sample molecules at time t . The factors for the overall detection efficiency, the molecular absorption cross-section, the fluorescence quantum yield, and the excitation intensity amplitude are assumed to be time-invariant, grouped together, and represented by the parameter ξ . For the assumption of a three-dimensional Gaussian probe volume, the normalized PSF can be written as $W(\vec{r}) = \exp[-2(x^2 + y^2)r_0^{-2} - 2z^2z_0^{-2}]$ where r_0 and z_0 are the radial and axial distance from the center to where the intensity has decayed by $1/e^2$, respectively.⁴⁸

The particle concentration $C(\vec{r}, t)$ can be described by the diffusion equation for a freely diffusing species:

$$\frac{\partial}{\partial t} C(\vec{r}, t) = D \nabla^2 C(\vec{r}, t) \quad (2)$$

where D is the diffusion coefficient and ∇^2 is the Laplace operator.

The normalized autocorrelation function for processes, which are both stationary and ergodic, is given by:⁴⁸

$$G(\tau) = \frac{\langle \delta F(0) \delta F(t) \rangle}{\langle F \rangle^2} \quad (3)$$

where $\langle \rangle$ denotes the time average.

Using the cylindrical-shaped volume approximation for the effective focal volume $V_{\text{eff}} = [\int \hat{W}(\vec{r}) dV]^2 [\int \hat{W}^2(\vec{r}) dV]^{-1}$, the diffusion time $\tau_D = r_0^2/4D$, the aspect ratio $\beta = r_0/z_0$, and the relation between the particle number N and the concentration $\langle N \rangle = V_{\text{eff}} \langle C \rangle$, Eq. 3 can be evaluated together with Eq. 1 and Eq. 2 to:⁴⁷

$$G(\tau) = \frac{1}{\langle N \rangle} \cdot \frac{1}{1 + \frac{\tau}{\tau_D}} \cdot \frac{1}{\sqrt{1 + \beta^2 \cdot \frac{\tau}{\tau_D}}} \quad (4)$$

Equation 4 is used to model the acquired FCS data. Once the diffusion coefficient of a molecule for a certain solvent is known, the hydrodynamic radius, which will give an estimate of the size of the molecule, can be calculated according to the Stokes–Einstein relation:⁴⁹

$$R_H = \frac{k_B T}{6\pi\eta_s D} \quad (5)$$

where k_B is the Boltzmann constant, T is the absolute temperature, and η_s is the viscosity of the solvent. This relationship was published by Einstein in 1905⁴⁹ in order to describe the movements of spherical particles with radius R_H suspended in a fluid due to Brownian motion. However, Eq. 5 can be applied for arbitrarily shaped particles,^{47,48} such as molecules for which R_H then describes an equivalent radius of a sphere with the same diffusion properties.

Figure 1 shows a schematic of the FCS microscope used in this project. The excitation light was provided by an air-cooled Ar ion laser from JDS Uniphase (model 2214-25ML) with a 25 mW multi-line laser head. The excitation laser beam (515 nm line) was connected to the optical train via a single-mode fiber and fiber couplers. If accurately aligned, a single-mode fiber allows only the propagation of a Gaussian TEM_{0,0} mode, creating a Gaussian beam shape at the output and serving as a spatial filter for the excitation light. The fluorescent light on the emission side of the setup was coupled into a multimode fiber with a core diameter of 50 μm , which substitutes for a 50 μm pinhole. The multi-mode fiber was coupled to a cubic beam splitter with each branch going to an avalanche photo diode (APD) (Pacer). The two APDs were cross-correlated yielding an improved signal. The maximum count rate for these single-photon-counting modules was 5 MHz with a dead time of 10 ns after each count. The optical train was built using components of the Microbench system (Linos), mounted on an optical breadboard. The microscope objective was a 60 \times oil immersion objective from Olympus with a transmittance greater than 85% in the relevant wavelength range between 500 nm and 700 nm. The filter set used in the FCS microscope consisted of a narrow band pass excitation filter for the 515 nm laser line (Edmund Optics), a dichroic (Chroma Technologies), and a Raman edge emission filter (CVI Laser).

The radial beam waist and the aspect ratio were determined from calibration measurements of quantum dots (QDs) to be $r_0 = 360$ nm and $\beta = 0.1$, respectively. The room temperature was monitored and kept constant at $T = 290$ K during the experiments; therefore the toluene viscosity was $\eta_s = 0.588$ cP at an ambient pressure of 14.7 psi. The diffusion times reported

Table II. Elemental composition and yield for coal-derived asphaltenes. The EA instrument does not achieve perfect mass balance, as each element is measured independently on an absolute scale.

	Resid yield wt%	wt%, dry					H:C Atomic ratio
		C	H	N	S	O (by difference)	
Coal-derived asphaltene							
Tanito Harum	24	90.56	5.59	2.11	0.1	1.64	0.74
Wyoming	25	89.41	6.04	1.43	0.13	2.99	0.81
Adaro	48	88.75	6.25	1.45	0.09	3.46	0.85
Petroleum asphaltene							
BG5	–	79.2	7.82	0.98	7.61	2.45 (measured)	1.18
UG8	–	81.07	7.11	1.02	8.94	1.6	1.05

here are somewhat shorter than those reported in a previous publication²² because the focal volume in the current set of experiments here was 16% smaller. To compensate for the change in focal volume, we have adjusted the diffusion times so that the diffusion constants in Table III agree with our previous measurements.²²

Each sample was measured for at least two different concentrations to increase the confidence in the acquired values. The typical concentrations used for the asphaltene samples were 230 µg/L and 2300 µg/L. In general, coverage of three orders of magnitude in concentration by the FCS microscope was possible, so a few samples were measured at concentrations between 23 µg/L and 2300 µg/L. Figure 2 shows an example of the raw (circles) and fitted data (solid lines) for the Violanthrone-78 dye. Equation 4 gives an excellent fit to the experimental data. Fits of comparable data quality were obtained for all samples.

Sample Preparation. Three kinds of coal liquefaction residues were used to obtain coal-derived asphaltenes. They originated from three different sub-bituminous coals: Adaro, Tanito Harum, and Wyoming coal. The Adaro coal liquefaction residue was obtained in the NEDOL 150 ton/day (t/d) pilot plant (PP), which was operated during 1996–1998 at Kashima City, Ibaraki, Japan.⁵⁰ The typical liquefaction conditions were the temperature 450–465 °C, the pressure 16.8 MPa (in part from added H₂), the gas to feed slurry ratio 0.7 Nm³/kg, and the coal concentration in feed slurry 40 wt%. The liquefaction residue was obtained from the resid in the vacuum distillation column where the liquefaction products were separated into

four fractions, i.e., the light oil fraction with boiling point below 220 °C, the medium oil fraction with boiling point ranging from 220 to 350 °C, the heavy oil fraction with boiling point ranging from 350 to 538 °C, and the liquefaction residue.

The liquefaction residues from Tanito Harum and Wyoming coals were obtained in the 1 t/d Process Supporting Unit (PSU) constructed for the support studies on the operations of the PP.⁵¹ The operating conditions and the process flow of the PSU are almost similar with those of the PP. The solid residues from distillation of the coal extracts were pulverized to pass through a 60-mesh screen and dried for 2 h under vacuum at 110 °C before use. The asphaltene fraction, which is toluene soluble and n-hexane insoluble, was obtained with the Soxhlet extraction technique. The yields as well as the elemental compositions of the asphaltene and oil samples are given in Table II.

RESULTS AND DISCUSSION

Figure 3 shows the FCS correlation curves for the Wyoming and Adaro coal-derived asphaltene fractions, two model compounds, and the UG8 and ST0 asphaltene. The correlation functions are scaled so that the initial amplitudes $G(0)$ are the same for all curves. As noted in the experimental section, all of these curves are exactly fit by the theoretical formalism, with no evidence of optical aberrations in the auto-correlation curve. The asphaltenes are essentially within the range of the model compounds. Generally, the diffusion coefficients decrease with increasing size but much less systematically with molecular

Table III. The translational diffusion times were obtained from least squares fits to the data using Eq. 4 as the fitting function. The diffusion coefficients were then derived from $\tau_D = r_0^2/4D$ and the hydrodynamic radii from Eq. 5. The excitation source was the 515 nm wavelength line from an Ar laser. The diffusion coefficients in Table III have been adjusted to agree with Ref. 22 (see text for explanation).

Sample name	Diffusion time τ_D ($\times 10^{-5}$ s)	Diffusion coefficient * D ($\times 10^{-6}$ cm ² /s)	Hydrodynamic radius R_H (Å)
WY-Coal-Derived Asphaltene	5.33	6.03	6.02
TH-Coal-Derived Asphaltene	5.23	6.15	5.91
TH-Coal-Derived Asphaltene (from Prof. Iino)	5.31	6.06	5.99
AD-Coal-Derived Asphaltene	5.48	5.87	6.19
CAL - Petroleum Asphaltene	8.14	3.95	9.19
UG8 - Petroleum Asphaltene	9.92	3.24	11.20
BG5 - Petroleum Asphaltene	9.96	3.23	11.25
STO - Petroleum Asphaltene	10.61	3.03	11.98
BPTD - Dye	5.47	5.88	6.18
BPHD -Dye	6.13	5.25	6.92
BPTI - Dye	6.37	5.05	7.19
Solar - Dye	6.40	5.02	7.23
PTP - Dye	6.73	4.78	7.60

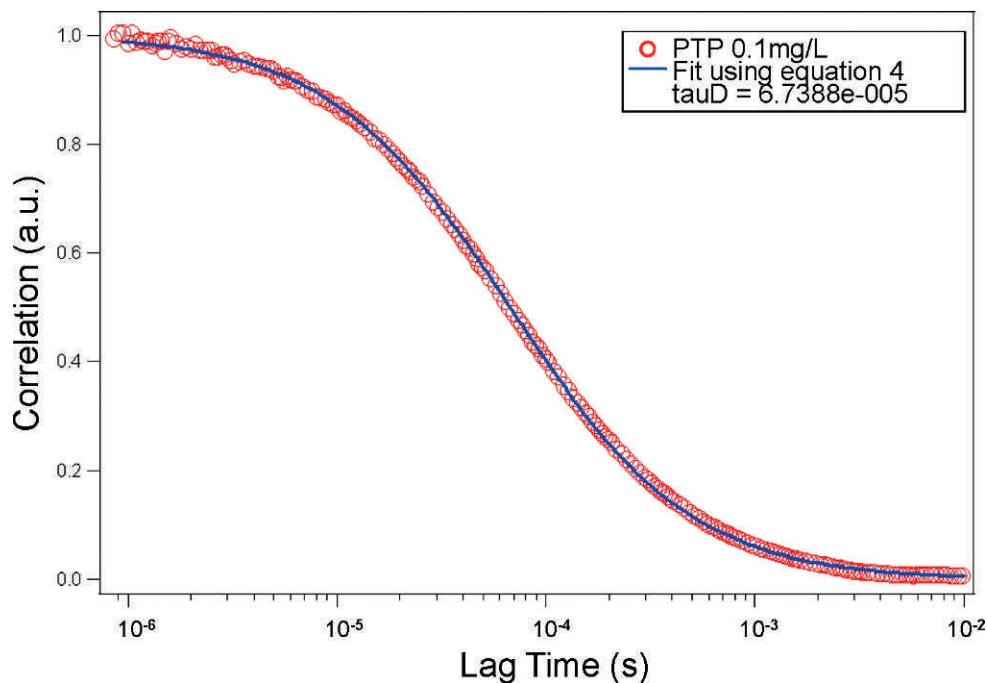


FIG. 2. FCS data (markers) and the corresponding theoretical fit (solid lines) for 0.1 mg/L concentration of Violanthrone-78, a perylene derivative. The experimental data and the corresponding fit (Eq. 4) are nearly indistinguishable. This allows us to accurately determine small differences in the diffusion constant D . The lag time is the correlation time t in the autocorrelation function (Eq. 4).

weight. Derived hydrodynamic radii are found to be smaller than the molecular geometry by a scaling prefactor f (~ 0.8) halfway between the stick ($f = 1$) and slip ($f = 2/3$) boundary conditions.⁵² In contrast TRFD depends on the rotational diffusion constant, which is very sensitive to the radius, scaling

as r^3 , and additionally the rotational diffusion constant is not very sensitive to the aspect ratio.³

Figure 3 clearly shows that for molecules of specific identical optical properties, the coal-derived asphaltenes all have very similar diffusion times, while the petroleum-

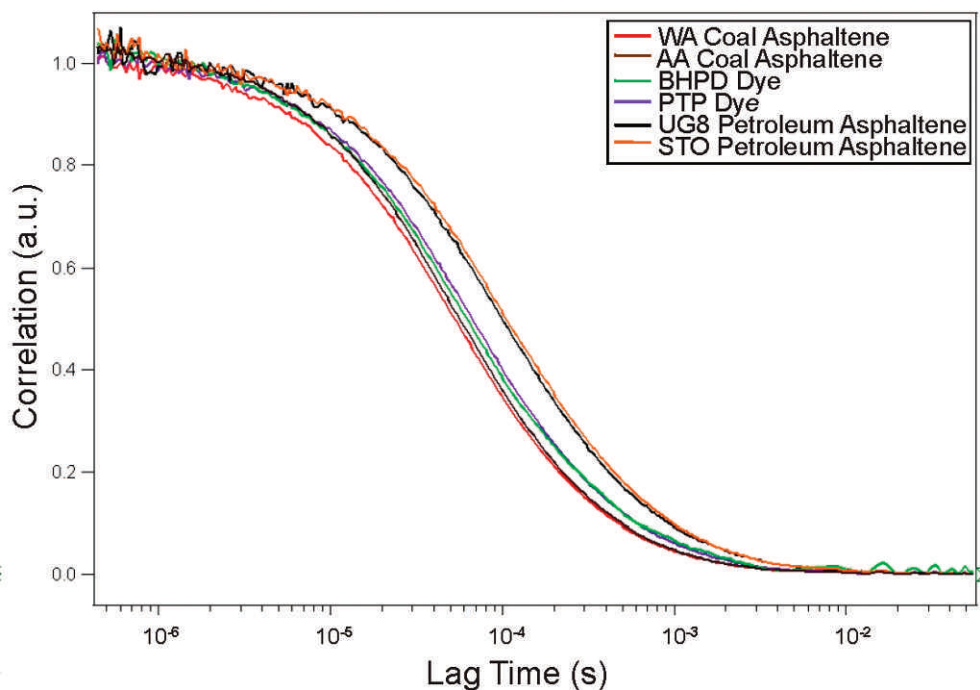


FIG. 3. FCS correlation decay curves for a coal-derived asphaltene fraction (WY, AA), two perylene derivative model compounds (BHPD and PTP), and two petroleum-derived asphaltenes (UG8, STO). The curves have been scaled along the y-axis for display purposes. The model compounds provide a reference for the range of possible asphaltene molecular sizes. The lag time is the correlation time t in the autocorrelation function (Eq. 4).

derived asphaltenes show more variation. It is important to remember that an optical constraint is imposed on the molecular fractions of asphaltenes being compared. For the FCS work herein, the constraint is that the molecular chromophores must absorb green light and fluoresce. Moreover, larger PAHs tend to absorb to the red.^{39–41} That is, there is a well-known correlation between PAH size and chromophore optical properties.

An important result seen in Fig. 3 is that the coal-derived asphaltene is much smaller than the petroleum-derived asphaltene. This was obtained previously for coal-derived asphaltene by TRFD using rotational diffusion.^{4,5,10} The fact that FCS and its translation diffusion measurement agree closely with TRFD means that internal rotational relaxation was not perturbing the TRFD results. Groups with pendant PAHs would be expected to exhibit some effects from internal rotational relaxation – if that rotational relaxation is sufficiently large. The comparison of FCS and TRFD shows rapid relaxation without internal rotational relaxation. Asphaltene molecules are small and without pendant PAHs. This is consistent with one or perhaps two PAHs per molecule. The translation and rotational diffusion constants have different dependencies on deviations from spherical structure. The single PAH of asphaltene molecules defines geometry. In addition, there are likely fused alicyclic rings attached to the PAH as determined from the presence of active hydrogen in asphaltenes.⁵³ The implications of this asymmetry are still being considered and may moderate some of the findings. In particular, the alicyclic rings on the petroleum asphaltenes might increase the translation diffusion constants somewhat to match model compounds with slightly larger PAHs.

Table III shows the FCS results obtained for several coals are indeed general and robust. Always, the coal-derived asphaltenes diffuse faster than the petroleum-derived asphaltenes. Somewhat different liquefaction processes were used for preparation of the different coal liquids but the asphaltene sizes are within 5% of each other, and thus there is very little variation. The diffusion constants of the two different preparations of the Tanito Harum coal-derived asphaltenes are almost identical. Table III also shows that many petroleum-derived asphaltenes exhibit comparable translational diffusion constants (again with the optical selection of green-induced fluorescence). And always, the petroleum asphaltene diffusion constants are much smaller, roughly half of those for the coal-derived asphaltenes. This is very consistent with the TRFD results^{4–7} as well as mass spectral results. In particular, well-controlled LDI experiments were performed on the TH asphaltene from Prof. Iino and on a petroleum asphaltene.³² The coal-derived asphaltene was reported to be $\sim 1/2$ the molecular weight of the petroleum asphaltene. This LDI study also concluded based on aggregation propensity that there must be a single large PAH in asphaltene molecules of relative low molecular weight.³² More recently L²MS mass spectroscopy has been performed on UG8 asphaltene and the Iino TH-coal-derived asphaltene. L²MS is very effective at removing concerns with asphaltene aggregation. The conclusion from this work is that the coal-derived asphaltene is half the molecular weight of UG8 asphaltene. The FCS results herein are in excellent agreement with previous diffusion and mass spectral results comparing petroleum- and coal-derived asphaltenes previously with a limited sample. The results here show these previous results are general.

COAL-DERIVED VERSUS PETROLEUM ASPHALTENES

Previously, it was noted that a coal-derived asphaltene had much less alkane carbon than petroleum asphaltene in concert with the much smaller alkane content of the source material coal over crude oil.¹⁰ An argument has been advanced that two primary molecular determinants control asphaltene energetics of solubility and must be balanced to give toluene solubility and heptane insolubility. Steric repulsion of alkane substituents must balance attractive van der Waals forces associated with PAHs. Steric repulsion of alkanes is known from basic chemistry principles even with regard to strongly impacting melting points of alkyl aromatics.¹⁰ The direct impact of alkane peripheral substituents on PAH solubility is known in the dye industry, as has been shown for alkyl-substituted hetero-PAHs relevant to asphaltenes.⁸ Moreover, the direct impact of disruption of order due to alkane substituents has been shown by transmission electron microscopy on model alkyl-substituted PAHs and petroleum and coal-derived asphaltenes.⁵⁴ The attractive effect of larger PAHs is well known in freshman organic chemistry laboratories, e.g., with the widespread use of decolorizing carbon trapping larger undesired reaction products. If net molecular repulsion is too large, the molecules become n-heptane soluble, and thus not asphaltenes, whereas if net molecular attraction is too large, toluene insolubility results. For example, in thermal decomposition, the alkanes are cracked off the rings, which reduces repulsion while the PAH attraction remains. The net effect is coke generation. Moreover, the cracking of alkanes off resins decreases solubility and this thermally modified fraction becomes asphaltenes of smaller molecular size, as has been observed.⁸

Here we test specific groups of chromophores (those with 515 nm induced fluorescence) and have shown that with this optical constraint, the corresponding coal-derived asphaltenes are half the molecular size compared to petroleum asphaltenes. We now explore the primary molecular structure differences. Table II shows the large difference in the H:C atomic ratio of all coal-derived samples versus the petroleum asphaltene. From our NMR measurements⁴³ we know that the petroleum asphaltene has 47% aromatic carbon while the coal-derived asphaltenes are close to 80% aromatic carbon. These substantial differences in aromatic to saturated carbon are seen to correlate very well with the diffusion constants listed in Table III. Thus, there is a sharp contrast between all coal-derived asphaltenes versus the petroleum asphaltene in both aromatic to saturated carbon and in terms of diffusion constant.

There are two components to this observation. First, for a given alkylated chromophore, loss of alkane carbon would reduce its diffusion constant. Again, for a given PAH chromophore, in going from a coal-derived asphaltene at 80% aromatic carbon to a petroleum asphaltene at 47% alkane carbon there is a 70% increase in total carbon. That is, the mass ratio would be 1.7 if linear in (alkane) carbon. For linear alkanes, the diffusion constant varies as $(n)^{0.7}$ where n is the carbon number.⁹ It is plausible that for a given chromophore the scaling of the diffusion constant is less than linear in alkane carbon. The trend in diffusion coefficients for the perylene derivatives suggests that the alkane chains contribute less than 25% to the diffusion constant. However, there is likely a second mechanism affecting the difference between the coal-derived and petroleum diffusion constants. Moreover, as noted above, it is likely that loss of this much alkane carbon would

significantly change the solubility characteristics of the compound. The second mechanism impacting relative diffusion constants is related to the differences in coal-derived vs. petroleum chromophores found in asphaltenes. Since the coal-derived asphaltenes have much less alkane carbon, it is likely that the corresponding chromophores within the asphaltene fraction are different and likely smaller than those of petroleum. Somewhat different sized chromophores can have similar optical properties.^{39–41}

Polar groups have a small but noticeable effect on asphaltene molecular size. The CAL asphaltene has an unusually high fraction of sulfoxide component (44% of its sulfur is alkyl sulfoxide).⁵⁵ The CAL asphaltene is “bidentate;” one site of attraction is the polar sulfoxide group, the second the PAH. To keep the overall binding energy in balance, the PAH and thus the CAL asphaltene molecules are somewhat smaller, as seen in Table III. This is consistent with previous TRFD findings for CAL asphaltene.⁵ This correlation between the PAH size and sulfoxide fraction follows only for the island molecular architecture. This repeated observation regarding CAL asphaltene and its sulfoxide is important support for the island molecular architecture. The oxygen functionality could play a secondary role in the difference between coal-derived vs. crude oil asphaltenes; the oxygen content is small in both cases and not dissimilar. Here we have compared a petroleum asphaltene with similar quantities of oxygen as the coal-derived asphaltenes (see Table II).

The large translational diffusion constants of the coal-derived asphaltenes are in concert with similar observations for petroleum samples.^{4,5} The implication is that there is no sharp contrast in molecular structure in going from coal asphaltene to petroleum asphaltene; rather, there is a continuum. This is especially true for asphaltene molecules with the same optical properties and thus very similar PAHs. Considering that these coal-derived materials are low molecular weight and that they have large chromophores that absorb green light, only one or perhaps two PAHs can fit within the molecular weight constraint. The claim that resins have multiple PAHs is not common, and the continuum of molecular properties shown here is consistent with the coal-derived asphaltenes having only one PAH.

CONCLUSIONS

Fluorescence correlation spectroscopy applied to several coal-derived asphaltenes has shown that the indications previously found regarding differences in coal-derived asphaltenes versus petroleum asphaltenes are indeed general and robust. In addition, the small differences in diffusion constants between asphaltenes with specific optical properties are found in coal-derived materials just as had previously been found with corresponding petroleum fractions, again with specific optical properties. Here, we establish the relationship between the small coal-derived asphaltenes, and their small aliphatic fraction is a general result. In particular, when specific chromophore properties are mandated as in these FCS experiments, the large diffusion constants of the coal-derived materials versus petroleum asphaltenes are still found. The comparison between coal-derived and petroleum asphaltenes offers the prospect of sorting out structure-function relationships in these materials. In particular, the central issue of the number of PAHs in asphaltene molecules can be addressed more readily in coal-derived asphaltenes than petroleum

asphaltenes because the former are half-size and have very little alkane, thereby issuing very tight constraints on molecular architecture.

NMR studies find the coal-derived asphaltenes have PAHs with 5 to 6 fused rings, while petroleum asphaltenes have PAHs with 6 to 7 fused rings. For coal-derived asphaltenes, the small molecular size, small alkane fraction, and large PAH all point to the dominance of the island molecular architecture. Dividing the coal PAH in half (for an archipelago of two islands) would yield colorless molecules; coal-derived asphaltenes are brown. A true archipelago model with multiple islands for coal asphaltene with its small alkane fraction would approach polystyrene, an unlikely proposal for a model of a coal asphaltene. For coal asphaltenes, the FCS data exhibits the small molecular size of coal-derived asphaltenes. These FCS translational diffusion results are shown herein to match closely with the TRFD rotational diffusion results. In addition, all unimolecular decomposition studies now being performed on asphaltenes are consistent with island molecular architecture. Fortunately, once again there is a confluence of conclusions from multiple, different methods addressing a major question in asphaltene science, whether the island molecular architecture is predominant in asphaltenes. Of course, these results do not rule out some asphaltene molecules with two or three PAHs.

ACKNOWLEDGMENT

We would like to thank H. Zheng for providing the BG5 sample.

1. O.C. Mullins, E.Y. Sheu, A. Hammami and A.G. Marshall, Eds., *Asphaltenes, Heavy Oils and Petroleomics* (Springer, New York, 2007).
2. O. C. Mullins, *Energy Fuels* **24**, 2179 (2010).
3. O. C. Mullins, *The Asphaltenes*, *Ann. Rev. of Anal. Chem.* **4**, 393 (2011).
4. H. Groenzin and O. C. Mullins, *J. Phys. Chem. A*, **103**, 11237 (1999).
5. H. Groenzin and O. C. Mullins, *Energy Fuels* **14**, 677 (2000).
6. E. Buenrostro-Gonzalez, H. Groenzin, C. Lira-Galeana, and O. C. Mullins, *Energy Fuels* **15**, 972 (2001).
7. L. Buch, H. Groenzin, E. Buenrostro-Gonzalez, S. I. Andersen, C. Lira-Galeana, and O. C. Mullins, *Fuel* **82**, 1075 (2003).
8. H. Groenzin, O. C. Mullins, S. Eser, J. Mathews, M.-G. Yang, and D. Jones, *Energy Fuels* **17**, 498 (2003).
9. S. Badre, C. Goncalves, K. Norinaga, G. Gustavson, and O. C. Mullins, *Fuel* **85**, 1 (2006).
10. V. J. Wargadalam, K. Norinaga, and M. Iino, *Fuel* **81**, 1403 (2002).
11. D. E. Freed, N. V. Lisitza, P. N. Sen, and Y.-Q. Song, in *Asphaltenes, Heavy Oils and Petroleomics*, O. C. Mullins, E. Y. Sheu, A. Hammami, and A. G. Marshall, Eds. (Springer, New York, 2007), Chap. 11, p. 279.
12. S. Goncalves, J. Castillo, A. Fernandez, and J. Hung, *Fuel* **83**, 1823 (2004).
13. G. Andreatta, N. Bostrom, and O. C. Mullins, *Langmuir* **21**, 2728 (2005).
14. G. Andreatta, C. C. Goncalves, G. Buffin, N. Bostrom, C. M. Quintella, F. Arteaga-Larios, E. Perez, and O. C. Mullins, *Energy Fuels* **19**, 1282 (2005).
15. E. Y. Sheu, Y. Long, and H. Hamza, in *Asphaltenes, Heavy Oils and Petroleomics*, O. C. Mullins, E. Y. Sheu, A. Hammami, and A. G. Marshall, Eds. (Springer, New York, 2007), Chap. 10, p. 259.
16. H. Zeng, Y. Q. Song, D. L. Johnson, and O. M. Mullins, *Energy Fuels* **23**, 1201 (2009).
17. L. Goual, *Energy Fuels* **23**, 2090 (2009).
18. L. Goual, M. Sedghi, H. Zeng, F. Mostowfi, R. McFarlane, and O. C. Mullins, *Fuel* (2011), paper accepted.
19. F. Mostowfi, K. Indo, O. C. Mullins, and R. McFarlane, *Energy Fuels* **23**, 1194 (2009).
20. A. B. Andrews, R. Guerra, P. N. Sen, and O. C. Mullins, *J. Phys. Chem. A* **110**, 8095 (2006).
21. R. Guerra, K. Ladavac, A. B. Andrews, P. N. Sen, and O. C. Mullins, *Fuel* **86**, 2016 (2007).
22. M. H. Schneider, A. B. Andrews, S. Mitra-Kirtley, and O. C. Mullins, *Energy Fuels* **21**, 2875 (2007).
23. M. M. Boduszynski, in *Chemistry Of Asphaltenes*, J. W. Bunger and N. C. Li, Eds. (American Chemical Society, Washington D.C., 1981), Chap. 7, pp. 119.

24. D. Zhan and J. B. Fenn, *Int. J. Mass Spectrom.* **194**, 197 (2000).
25. R. P. Rodgers and A. G. Marshall, in *Asphaltenes, Heavy Oils and Petroleomics*, O. C. Mullins, E. Y. Sheu, A. Hammami, and A. G. Marshall, Eds. (Springer, New York, 2007), Chap. 3, p. 63.
26. G. C. Klein, S. Kim, R. P. Rodgers, A. G. Marshall, A. Yen, and S. Asomaning, *Energy Fuels* **20**, 1965 (2006).
27. J. M. Purcell, C. L. Hendrickson, P. Dunk, H. W. Kroto, and A. G. Marshall, Proceedings of the 55th American Society For Mass Spectrometry Annual Conference On Mass Spectrometry (Indianapolis, IN, 3–7 June 2007), Poster MPD068.
28. O. C. Mullins, B. Martinez-Haya, and A. G. Marshall, *Energy Fuels* **22**, 1765 (2008).
29. A. A. Herod, K. D. Bartle, and R. Kandiyoti, *Energy Fuels* **21**, 2176 (2007).
30. A. R. Hortal, B. Martinez-Haya, M. D. Lobato, J. M. Pedrosa, and S. Lago, *J. Mass Spectrom.* **41**, 960 (2006).
31. B. Martinez-Haya, A. R. Hortal, P. M. Hurtado, M. D. Lobato, and J. M. Pedrosa, *J. Mass Spectrom.* **42**, 701 (2007).
32. A. R. Hortal, P. M. Hurtado, B. Martinez-Haya, and O. C. Mullins, *Energy Fuels* **21**, 2863 (2007).
33. A. E. Pomerantz, M. R. Hammond, A. L. Morrow, O. C. Mullins, and R. N. Zare, *J. Am. Chem. Soc.* **130**, 7216 (2008).
34. A. E. Pomerantz, M. R. Hammond, A. L. Morrow, O. C. Mullins, and R. N. Zare, *Energy Fuels* **23**, 1162 (2009).
35. H. Sabbah, A. L. Morrow, A. E. Pomerantz, and R. N. Zare, *Energy Fuels* **25**, 1597 (2011).
36. D. S. Pinkston, P. Duan, V. A. Gallardo, S. C. Habicht, and X. Tan, et al., *Energy Fuels* **23**, 5564 (2009).
37. D. Borton, D. S. Pinkston, M. R. Hurt, X. Tan, and K. Azyat, et al. *Energy Fuels* **24**, 5548 (2010).
38. R. P. Rodgers, X. Tan, B. M. Ehrmann, P. Juyal, A. M. McKenna, J. M. Purcell, T. M. Schaub, M. R. Gray, and A. G. Marshall, *9th Int'l Conf. On Petroleum Phase Behavior & Fouling* (Victoria, B.C., Canada, 15–19 June, 2008), Abstract #102.
39. Y. Ruiz-Morales and O. C. Mullins, *Energy Fuels* **21**, 256 (2007).
40. Y. Ruiz-Morales, X. Wu, and O. C. Mullins, *Energy Fuels* **21**, 944 (2007).
41. Y. Ruiz-Morales and O. C. Mullins, *Energy Fuels* **23**, 1169 (2009).
42. A. B. Andrews, A. McClelland, O. Korkeila, A. Demidov, A. Krummel, O. C. Mullins, and Z. Chen, *Langmuir* **27**, 6049 (2011).
43. A. B. Andrews, J. C. Edwards, D. Pomerantz, O. C. Mullins, and K. Norinaga, *Energy Fuels* **25**, 3068 (2011).
44. T. Dittmar, *Org. Geochem.* **39**, 396 (2008).
45. B. P. Koch and T. Dittmar, *Rapid Commun. Mass Spectrom.* **20**, 926 (2006).
46. T. Dittmar and B. P. Koch, Thermogenic organic matter dissolved in the abyssal ocean, *Mar. Chem.* **102**, 208 (2006).
47. P. Schwille and E. Haustein, *Biophysics Textbook Online* (www.biophysics.org/btol/) (January 2007).
48. D. C. Lamb, *Lecture Notes On Fluctuation Spectroscopy* (Department of Physical Chemistry, Ludwig-Maximilian-Universität (LMU), Munich, 2004).
49. A. Einstein, *Annalen Der Physik* **322**, 549 (1905).
50. K. Hirano, *Fuel Proc. Technol.* **62**, 2 109 (2000).
51. K. Ikeda, K. Sakawaki, and Y. Nogami, et al., *Fuel* **79**, 3 373 (2000).
52. P. J. Espinosa and J. G. de la Torre, *J. Phys. Chem.* **91**, 3612 (1987).
53. K. A. Gould and I. A. Wiehe, *Energy Fuels* **21**, 1199 (2007).
54. A. Sharma, H. Groenzin, O. C. Mullins, and A. Tomita, *Energy Fuels* **16**, 2 (2002).
55. S. Mitra-Kirtley, O. C. Mullins, C. Y. Ralston, D. Sellis, and C. Pareis, *Appl. Spectrosc.* **52**, 12 (1998).